11314 *Inorg. Chem.* **2009**, *48*, 11314–11324
DOI: 10.1021/ic9018103

Inorganic Chemistry
Article

Molecular Conductors Based on the Mixed-Valence Polyoxometalates $[SMo_{12}O_{40}]^{n-}$ (n = 3 and 4) and the Organic Donors Bis(ethylenedithio)tetrathiafulvalene and Bis(ethylenedithio)tetraselenafulvalene

Eugenio Coronado,[†] Simona Curreli,[†] Carlos Giménez-Saiz,*[,†,‡] Carlos J. Gómez-García,*[,†] Antonio Alberola,[§] and Enric Canadell[∥]

[†]*Institute of Molecular Science (ICMol), Scientific Park and* [‡]*Fundació General de la Universitat de València and University of Valencia, P.O. Box 22085, 46071 Valencia, Spain,* [§]*Dpto. de Química Física y Analítica, University Jaume I, Avda. Sos Baynat s/n, 12701 Castellón, Spain, and* [∥]*Institut de Ciencia de Materials de Barcelona (ICMAB), CSIC, Campus de la UAB, 08193 Bellaterra, Spain*

Received September 11, 2009

The synthesis, crystal structure, and physical characterization of two new radical salts formed by the organic donors bis(ethylenedithio)tetrathiafulvalene (ET) and bis(ethylenediseleno)tetrathiafulvalene (BETS) and the Keggin polyoxometalate (POM) $[SMo_{12}O_{40}]^{n-}$ are reported. The salts isolated are $ET_8[SMo_{12}O_{40}]\cdot 10H_2O$ (**1**) (crystal data: (**1**) monoclinic, space group $I2/m$ with a = 13.9300(10) Å, b = 43.467(3) Å, c = 13.9929(13) Å, β = 107.979(6)°, V = 8058.9(11) Å^3, Z = 2) and $BETS_8[SMo_{12}O_{40}]\cdot 10H_2O$ (**2**) (crystal data: monoclinic, space group $I2/m$ with a = 14.0878(2) Å, b = 44.1010(6) Å, c = 14.0930(2) Å, β = 106.739(3)°, V = 8384.8 Å^3, Z = 2). Both compounds are isostructural and consist of alternating layers of the organic donors (with an α or θ_{42+40} packing mode) and POM anions. The structural data, as well as the magnetic susceptibility, ESR measurements, and band structure calculations, indicate that the Keggin POMs have been reduced by one electron in **1** and by two electrons in **2**, leading to the POMs $[SMo_{12}O_{40}]^{3-}$ and $[SMo_{12}O_{40}]^{4-}$ in **1** and **2**, respectively. At ambient pressure **1** is a classical semiconductor with a room temperature conductivity of about 1 S cm^{-1} and an activation energy of about 130 meV. Salt **2** also exhibits an activated behavior although it does not follow a classical semiconducting regime. The conductivity of **2** under applied pressure shows an enhanced conductivity, in agreement with the analysis of the electronic structure, although no metallic behavior is detected below about 10 kbar.

Introduction

In the past years, polyoxometalate (POM) anions have been combined with π-electron donors derived from the tetrathiafulvalene (TTF) or perylene (per) molecules giving rise to a wide family of organic−inorganic hybrid molecular materials having insulating, semiconducting, or even metallic behavior.[1] Because of the presence of POM, these charge transfer salts also exhibited unusual structural and/or electronic features arising from the unique properties of POM anions (bulky sizes, highly symmetrical shapes, high charges, ability to act as electron acceptors and to include 3d magnetic ions, and so forth). However, the observation of a metallic state in these materials has been very scarce mainly because of the charge localization induced in the organic sublattice by the high charges of the polyanions and the irregular donor stacking provoked by their bulkiness. In fact, the only example exhibiting metallic behavior down to 2 K is the radical salt $BEDO_6K_2[BW_{12}O_{40}]\cdot 11H_2O$, that shows a room temperature conductivity of 37 S cm^{-1} and the highest conductivity observed to date for a POM-containing radical salt (910 S cm^{-1} at 2 K).[2] The other scarce examples of metallic radical salts containing POM are as follows: $ET_5[H_3V_{10}O_{28}]\cdot 4H_2O$ (metallic down to 50 K),[3] $ET_6[Mo_8O_{26}]\cdot(DMF)_3$ (metallic down to 60 K),[4] and $ET_{11}[P_2W_{18}O_{62}]\cdot 3H_2O$ and $ET_5[VW_5O_{19}]\cdot 6H_2O$ (both metallic down to ca. 250 K).[5,6]

*To whom correspondence should be addressed. E-mail: carlos.gimenez@uv.es (C.G.-S.), carlos.gomez@uv.es (C.J.G.-G.).

(1) Coronado, E.; Gómez-García, C. J. *Chem. Rev.* **1998**, *98*, 273. (b) Coronado, E.; Giménez-Saiz, C.; Gómez-García, C. J. *Coord. Chem. Rev.* **2005**, *249*, 1776.

(2) Coronado, E.; Giménez-Saiz, C.; Gómez-García, C. J.; Capelli, S. C. *Angew. Chem., Int. Ed.* **2004**, *43*, 3022.

(3) Coronado, E.; Galán-Mascarós, J. R.; Giménez-Saiz, C.; Gómez-García, C. J.; Martínez-Ferrero, E.; Almeida, M.; Lopes, E. B. *Adv. Mater.* **2004**, *16*, 324.

(4) Łapiński, A.; Starodub, V.; Golub, M.; Kravchenko, A.; Baumer, V.; Faulques, E.; Graja, A. *Synth. Met.* **2003**, *138*, 483.

(5) (a) Coronado, E.; Galán-Mascarós, J. R.; Giménez-Saiz, C.; Gómez-García, C. J.; Laukhin, V. N. *Adv. Mater.* **1996**, *8*, 801. (b) Coronado, E.; Clemente-León, M.; Galán-Mascarós, J. R.; Giménez-Saiz, C.; Gómez-García, C. J.; Martínez-Ferrero, E. *J. Chem. Soc., Dalton Trans.* **2000**, 3955.

(6) Triki, S.; Ouahab, L.; Grandjean, D.; Canet, R.; Garrigou-Lagrange, C.; Delhaès, P. *Synth. Met.* **1993**, *56*, 2028.

 Published on Web 10/29/2009

This short number of examples of metallic POM-containing radical salts demonstrates that the synthesis of new metallic radical salts with POM still remains a challenge. Interestingly, except in the radical salt $ET_{11}[P_2W_{18}O_{62}]\cdot 3H_2O$[5] (where the POM charge is −6) the anionic charge in all these examples is relatively low (−3 and −4), suggesting that low charge POMs are better candidates to obtain metallic radical salts.

The most used and studied POMs are those with the Keggin structure and formula $[XM_{12}O_{40}]^{n-}$, providing the most extensive series of isostructural compounds formulated as ET_8[Keggin]·solvent and ET_6[Keggin]·solvent.[7] In this family the itinerant electrons in the organic sublattice can coexist with a variety of situations in the inorganic network depending on the particular Keggin POM employed (which can be diamagnetic, contain a paramagnetic heteroatom, and/or be reduced by one electron). All these materials showed semiconducting behaviors (with room temperature conductivities of about $10^{-1}-10^{-2}$ S cm^{-1} and activation energies of about 100−150 meV), regardless of the charge in the organic sublattice (that can be varied from −3 to −6). Surprisingly, band structure calculations[7c] predict a semiconducting behavior when this charge is −4 or −6 (as in the derivatives with X = Si^{IV}, Co^{II}, Cu^{II}, and $2H^+$) but a metallic character when the charge is −5 (as in the derivatives with X = Fe^{III} and B^{III}). This disagreement is certainly related with the existence of different ET molecules in the solids as a consequence of the inhomogeneous charge distribution, which leads to different site energies and so to a charge localization. Nevertheless, this series clearly evidence another advantage of the use of POMs in radical salts: the possibility of varying the electronic band filling of the organic sublattice (and therefore the physical properties) by changing the charge of the polyoxoanion (if the crystal structure of the radical salt is retained). This very unusual feature in radical salts has been achieved in the isostructural radical salts of perylene (per): $(per)_5[M_6O_{19}]$, (M = Mo, W) and $(per)_5[VW_5O_{19}]$ which contain Lindquist POMs with the same size and shape but different anionic charges (−2 and −3, respectively).[8] This change in the anionic charge led to marked differences in the transport (hole or electron dominated conduction) and magnetic properties (diamagnetic or paramagnetic).[8,9] All these previous results suggest that a possible way to improve the electrical conductivity in the series ET_8[Keggin] (while keeping the crystal structure) could be the tuning of its band filling by using Keggin POMs with charges other than −4, −5, or −6 (already used). Although more scarce, there are some Keggin polyoxoanions as $[PMo_{12}O_{40}]^{3-}$ and $[SMo_{12}O_{40}]^{2-}$ that bear lower charges and therefore, may be used as anionic components of radical salts with ET to improve the electrical properties. Furthermore, these Mo-containing Keggin POMs are easy to reduce by one or two electrons, leading to mixed valence heteropolyblues and can, therefore, change their charge in one or two units.[7e,10] An additional way to improve the electrical conductivity in the series ET_8[Keggin] without changing the crystal structure consists of modifying the organic sublattice by using an analogous seleno-substituted ET molecule. Selenium has more extended π orbitals than sulfur, favoring a larger intermolecular HOMO−HOMO overlap and therefore a stabilization of the metallic state at low temperatures.[11] This strategy was tested with the donor bis(ethylenediseleno)tetrathiafulvalene (BEST) and the Keggin polyoxoanion $[PMo_{12}O_{40}]^{3-}$, giving rise to a radical salt of formula $(BEST)_3H[PMo_{12}O_{40}]\cdot CH_3CN\cdot CH_2Cl_2$ that showed a different crystal structure where the donors do not form stacks with overlapping π orbitals, but isolated molecules and dimers, leading to a lack of mixed-valence character in the organic part.[12] A better candidate should be the bis(ethylenedithio)tetraselenafulvalene (BETS) donor because the Se atoms in the central TTF skeleton can establish more intermolecular transverse interactions than the BEST donor, favoring the formation of radical salts with similar organic packing and crystal structures as the ET salts. In fact, most radical salts of the BETS donor exhibit metallic behavior down to low temperatures, including several superconductors.[11]

To take advantage of both factors (Keggin POM with low charges and Se-containing donors), we have prepared two new radical salts with the donors ET and BETS and the Keggin POM $[SMo_{12}O_{40}]^{n-}$ (n = −3 and −4): $ET_8[SMo_{12}O_{40}]\cdot 10H_2O$ (**1**) and $BETS_8[SMo_{12}O_{40}]\cdot 10H_2O$ (**2**). Here we report the synthesis, crystal structures, solid state properties, and band structure calculations of these two new radical salts.

Experimental Section

Synthesis. The organic donor bis(ethylenedithio)-tetrathiafulvalene (ET) was purchased from Fluka and used as received. The donor BETS was synthesized as described in the literature.[13] The POM salt $[NHex_4]_2[SMo_{12}O_{40}]$ ($NHex_4^+$ = tetrahexylammonium) was also prepared as previously reported.[10] Acetonitrile (Fluka, 99%) and dichloromethane (Fluka, 99%) were used as received. Radical salts **1** and **2** were prepared by electrochemical oxidation of the donor on platinum wire electrodes in U-shaped cells under low constant current. The anodic and cathodic compartments are separated by a porous glass frit. The exact conditions for the synthesis of each particular radical salt are described below.

Synthesis of $ET_8[SMo_{12}O_{40}]\cdot 10H_2O$ (1). A stirred suspension of $[NHex_4]_2[SMo_{12}O_{40}]$ (200 mg) in 15 mL of dichloromethane and 5 mL of acetonitrile was distributed between the two compartments of a U-shaped cell. Solid ET (8 mg) was introduced in the anode compartment, and the mixture was stirred

(7) (a) Gómez-García, C. J.; Ouahab, L.; Giménez-Saiz, C.; Triki, S.; Coronado, E.; Delhaès, P. *Angew. Chem., Int. Ed. Engl.* **1994**, *33*, 223. (b) Galán-Mascarós, J. R.; Giménez-Saiz, C.; Triki, S.; Gómez-García, C. J.; Coronado, E.; Ouahab, L. *Angew. Chem., Int. Ed. Engl.* **1995**, *34*, 1460. (c) Gómez-García, C. J.; Giménez-Saiz, C.; Triki, S.; Coronado, E.; Le Magueres, P.; Ouahab, L.; Ducasse, L.; Sourisseau, C.; Delhaès, P. *Inorg. Chem.* **1995**, *34*, 4139. (d) Coronado, E; Galán-Mascarós, J. R.; Giménez-Saiz, C.; Gómez-García, C. J.; Triki, S. *J. Am. Chem. Soc.* **1998**, *120*, 4671. (e) Kurmoo, M.; Bonamico, M.; Bellitto, C.; Fares, V.; Federici, F.; Guionneau, P.; Ducasse, L.; Kitagawa, H.; Day, P. *Adv. Mater.* **1998**, *10*, 545. (f) Davidson, A.; Boubekeur, K.; Penicaud, A.; Auban, P.; Lenoir, C.; Batail, P.; Herve, G. *J. Chem. Soc., Chem. Commun.* **1989**, 1373.

(8) Clemente-León, M.; Coronado, E.; Giménez-Saiz, C.; Gómez-García, C. J.; Martínez-Ferrero, E.; Almeida, M.; Lopes, E. B. *J. Mater. Chem.* **2001**, *11*, 2176.

(9) (a) Mori, T. *Chem. Rev.* **2004**, *104*, 4947. (b) Perruchas, S.; Boubekeur, K.; Canadell, E.; Misaki, Y.; Auban-Senzier, P.; Pasquier, C.; Batail, P. *J. Am. Chem. Soc.* **2008**, *130*, 3335.

(10) Vu, T.; Bond, A. M.; Hockless, D. C. R.; Moubaraki, D.; Murray, K. S.; Lazarev, G.; Wedd, A. G. *Inorg. Chem.* **2001**, *40*, 65.

(11) Kobayashi, H.; Cui, H.; Kobayashi, A. *Chem. Rev.* **2004**, *104*, 5265.

(12) Coronado, E.; Galán-Mascarós, J. R.; Giménez-Saiz, C.; Gómez-García, C. J.; Falvello, L. R.; Delhaès, P. *Inorg. Chem.* **1998**, *37*, 2183.

(13) Courcet, T.; Malfant, I.; Pokhodnia, K.; Cassoux, P. *New J. Chem.* **1998**, *22*, 585.

for 1 h more and then allowed to settle during 24 h. After this period, 4 drops of water were added to the anode compartment, and a constant current of 1 μA was applied. Black shiny elongated plates were collected from the platinum anode after 20 days.

Synthesis of $BETS_8[SMo_{12}O_{40}]\cdot 10H_2O$ (2). A stirred suspension of $[NHex_4]_2[SMo_{12}O_{40}]$ (200 mg) in 15 mL of dichloromethane and 5 mL of acetonitrile was distributed between the two compartments of a U-shaped cell. Solid BETS (8 mg) was introduced in the anode compartment, and the mixture was stirred for 1 h more and then allowed to settle during 24 h. After this period, 4 drops of water were added to the anode compartment, and a constant current of 1 μA was applied. Black shiny elongated plates were collected from the platinum anode after 20 days.

Structure Determination. The crystal structures of compounds **1** and **2** were determined from single crystal X-ray diffraction data collected at 292(2) K. Data were collected with a Nonius KappaCCD diffractometer using a graphite monochromated Mo Kα radiation source (λ = 0.71073 Å). Denzo and Scalepack[14] programs were used for cell refinements and data reduction. The structures were solved by direct methods using the SIR97[15] program with the WinGX[16] graphical user interface. The structure refinements were carried out with SHELX-97.[17] A multiscan absorption correction, based on equivalent reflections, was applied to the data using the program SORTAV.[18] All non-hydrogen atoms were refined anisotropically with the exception of the disordered carbon atoms of one of the ethylene groups in one donor molecule of **2**. Hydrogen atoms on carbon atoms were included at calculated positions and refined with a riding model. Hydrogen atoms of water molecules were not located. Crystal data are shown in Table 1.

Conductivity Measurements. Direct current (dc) conductivity measurements over the temperature range 2−300 K were performed with the four contacts method for several single crystals of each salt, giving reproducible results in all the samples. The contacts between the platinum wires (25 μm diameter) and the samples were done using graphite paste. All the samples were measured with cooling and warming rates of 1 K min^{-1} and with dc intensity currents of 1 μA in a Quantum Design PPMS-9. The results in the cooling and warming scans where identical, within experimental error, except for small microcracks observed in some of the crystals. The dc conductivity measurements under pressure were performed with a homemade pressure cell applying hydrostatic pressure with silicone-300 oil. The pressure inside the cell was measured with a previously calibrated manganin resistance.

Magnetic Measurements. Variable temperature susceptibility measurements were carried out in the temperature range 2−300 K with an applied magnetic field of 0.5 T on polycrystalline samples of **1** and **2** with a Quantum Design MPMS-XL-5 SQUID magnetometer. ESR spectra were recorded in X band for salt **1** (ν = 7.79 GHz) and Q-band (ν = 34.0 GHz) for salt **2** with a Bruker ELEXSYS E-500 Spectrometer in the temperature range 300−3 K on polycrystalline samples of both salts.

Band Structure Calculations. The tight-binding band structure calculations were based upon the effective one-electron Hamiltonian of the extended Hückel method.[19] The off-diagonal matrix elements of the Hamiltonian were calculated according to the modified Wolfsberg−Helmholz formula.[20] All valence electrons were explicitly taken into account in the calculations, and the basis set consisted of double-ζ Slater-type orbitals for C, S, and Se and single-ζ Slater-type orbitals for H. The exponents, contraction coefficients, and atomic parameters for C, S, Se, and H were taken from previous work.[21,22]

Table 1. X-ray Crystallographic Data for $ET_8[SMo_{12}O_{40}]\cdot 10H_2O$ (**1**) and $BETS_8[SMo_{12}O_{40}]\cdot 10H_2O$ (**2**)

	1	**2**
chemical formula	$C_{80}H_{84}Mo_{12}O_{50}S_{65}$	$C_{80}H_{84}Mo_{12}O_{50}S_{33}Se_{32}$
fw	5080.65	6581.45
cryst syst	monoclinic	monoclinic
space group	*I*2/*m*	*I*2/*m*
a (Å)	13.9300(10)	14.0878(2)
b (Å)	43.467(3)	44.1010(6)
c (Å)	13.9929(13)	14.0930(2)
β (deg)	107.979(6)	106.739(3)
V (Å^3)	8058.9(11)	8384.8(2)
T/K	292(2)	292(2)
Z	2	2
ρ_{calcd}/g cm^{-3}	2.094	2.607
μ/mm^{-1}	1.816	8.293
$R(F_o)$, $R_w(F_o^2)$ $[I < 2\sigma(I)]^a$	0.0850, 0.1996	0.0660, 0.1821

$^a R = \sum||F_o| - |F_c||/\sum|F_o|$; $R_w = \{\sum w(F_o^2 - F_c^2)^2/\sum w(F_o^2)^2\}^{1/2}$.

Results and Discussion

Synthesis. As mentioned in the introduction, an extensive series of radical salts with the general formula ET_8-[Keggin]·solvent can be obtained combining Keggin POMs and the ET donor.[7] These radical salts can crystallize in three different, but closely related, structures having the α-type packing mode (θ_{42+40} in Mori's notation)[23] in the organic sublattice. These three closely related θ_{42+40} or α-type structures are denoted as α_1, α_2, and α_3 (see Figure 1).[7] The α_1 and α_2 phases can be selectively prepared using most non-substituted Keggin polyoxoanions by carefully modifying the experimental conditions of synthesis: the α_1 phase is obtained when a mixture of CH_2Cl_2 and CH_3CN in the 3:1 ratio is used as solvent in the electro-crystallization cell, while the α_2 phase is obtained with a mixture of the same solvents in a 1:1 ratio. This strategy works well for the Keggin anions $[XW_{12}O_{40}]^{n-}$ (X = Co^{II}, Cu^{II}, Fe^{III}, $2H^+$). In the case of the polyoxoanion $[SMo_{12}O_{40}]^{2-}$ both synthetic conditions have been tested, leading in all cases to the α_1 phase for both donors, ET and BETS. Therefore, it seems that the $[SMo_{12}O_{40}]^{2-}$ POM, probably because of its lower charge, does not behave as the other tested Keggin POMs.

Crystal Structures of $ET_8[SMo_{12}O_{40}]\cdot 10H_2O$ (1) and $BETS_8[SMo_{12}O_{40}]\cdot 10H_2O$ (2). Compounds **1** and **2** are isostructural as found by the determination of their structures by single-crystal X-ray analysis. Table 1 contains the relevant crystallographic data and collection parameters. Figure 2 shows a standard Oak Ridge

(14) Otwinowski, Z.; Minor, W. DENZO-SCALEPACK, Processing of X-ray Diffraction Data Collected in Oscillation Mode. In *Methods in Enzymology, Volume 276, Macromolecular Crystallography, Part A*; Carter, C. W., Jr., Sweet, R. M., Eds.; Academic Press: New York, 1997.
(15) Altomare, A.; Burla, M. C.; Camalli, M.; Cascarano, G.; Giacovazzo, C.; Guagliardi, A.; Moliterni, A. G. G.; Polidori, G.; Spagna, R. *J. Appl. Crystallogr.* **1999**, *32*, 115.
(16) Farrugia, L. J. *J. Appl. Crystallogr.* **1997**, *32*, 837.
(17) Sheldrick, G. M. *SHELX-97*; University of Göttingen: Göttingen, Germany, 1997.
(18) Blessing, R. H. *J. Appl. Crystallogr.* **1997**, *30*, 421.
(19) Whangbo, M. H.; Hoffmann, R. *J. Am. Chem. Soc.* **1978**, *100*, 6093.
(20) Ammeter, J.; Bürgi, H.-B.; Thibeault, J.; Hoffmann, R. *J. Am. Chem. Soc.* **1978**, *100*, 3686.
(21) Pénicaud, A.; Boubekeur, K.; Batail, P.; Canadell, E.; Auban-Senzier, P.; Jérome, D. *J. Am. Chem. Soc.* **1993**, *115*, 4101.
(22) Pénicaud, A.; Batail, P.; Coulon, C.; Canadell, E.; Perrin, C. *Chem. Mater.* **1990**, *2*, 123.
(23) Mori, T.; Mori, H.; Tanaka, S. *Bull, Chem. Soc. Jpn.* **1999**, *72*, 179.

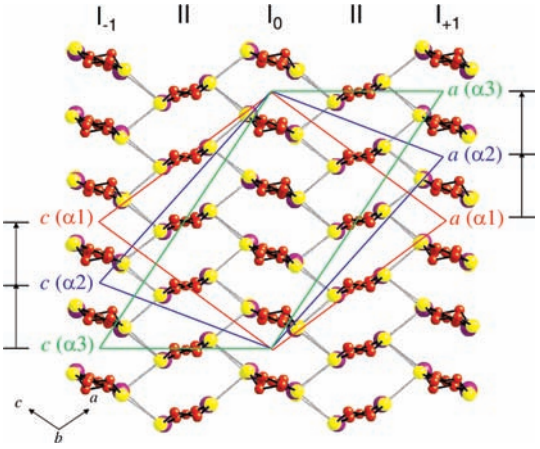

Figure 1. View of the organic layer of the three α phases in the *ac* plane showing the relation between them. The Keggin POM are located in the corners and the center of the unit cells. The arrows indicate the displacements that the POM (and the organic molecules of the type I chains) undergo to transform the α_1 phase into the α_2 or α_3 phases.

thermal ellipsoid plot (ORTEP)[24] diagram of the molecules of **1** and **2** with 50% thermal ellipsoids and atom numbering scheme. The unit cell parameters of compounds **1** and **2** correspond to the so-called α_1 phase.[7] The larger *b* parameter and unit cell volume of **2**, compared to **1**, are due to the larger molecular size of BETS compared to the ET donor.

Both structures consist of layers of the organic donors and the inorganic Keggin POM perpendicular to the *b* axis (Figure 3). There are three crystallographically different donor molecules (denoted as A, B, and C) which arrange forming two different types of stacks that alternate in the [10$\bar{1}$] direction and run in the [101] direction (Figure 4). One of the stacks (labeled II in Figures 1 and 3) is formed by alternated B and C donor molecules packed in an eclipsed way while the other stack (labeled I in Figures 1 and 3) is formed by dimers of A molecules that are displaced along the central C=C bond by one external ring of the donor molecule, giving rise to a zigzag chain of dimers (see Figure 4). Therefore, there are four donors of type A, two of type B, and two of type C per formula in **1** and **2**. The most obvious structural differences between **1** and **2** are found in the number and type of chalcogen···chalcogen intermolecular contacts shorter than the sum of the van der Waals radii (see Table 2). In **1** and **2** all these contacts are found between molecules belonging to different stacks only (interstack contacts). In **1** there are not short contacts involving chalcogens of the fulvalene moieties while in **2** there are three of such contacts (see Table 2 and arrows in Figure 3). Considering now the short intermolecular contacts involving chalcogens of fulvalene moieties and sulfur atoms of dihydrodithiin rings, one finds five of such contacts that are common to **1** and **2** and two additional contacts in **2** that are not found in **1** (see Table 2). Finally, a similar number of short contacts involving only sulfur atoms of dihydrodithiin rings are found in **1** and **2** (seven and six of such contacts, respectively). Therefore, despite that **1** and **2** are isostructural, the presence of BETS molecules in **2** gives rise to a larger number of intermolecular contacts shorter than the sum of the van der Waals radii, particularly between the fulvalene moieties of the donors. This is due to the larger van der Waals radii of selenium compared to sulfur and renders **2** a better candidate than **1** for the stabilization of the metallic state at low temperatures.

An estimate of the ionic charges on the ET molecules in **1** can be made from the known correlations between the intramolecular distances of the fulvalene moiety and the oxidation degree.[25] Such estimate indicates that the ET molecules of A and C types have a charge of about +1/2, while B molecules are almost neutral. As there are four molecules of type A and two molecules of type B and C per formula, the total positive charge is close to +3, indicating that the polyoxomolybdate has been reduced by one electron during the electrocrystallization process, bearing a total charge of −3. Even reduced, the POM $[SMo_{12}O_{40}]^{3-}$ represents the lowest anionic charge borne by a Keggin POM in the extended series of radical salts ET_8[Keggin]·solvent (the lowest charge to date was −4).[7] This result confirms the ability of POMs to tune the electronic band filling in the organic sublattice while maintaining the crystal structure. In addition, until now the only member of the family ET_8[Keggin]·solvent containing a one-electron reduced POM was $ET_8[PMo_{12}O_{40}]$·solvent (with an anionic charge of −4).[26]

Since there are no complete studies of the charge-bond lengths relationship in the BETS molecules, an estimation of the ionic charges on the BETS molecules in salt **2** can only be made by comparison with the bond lengths of the BETS donors in other radical salts in which the charge of the donors can be unambiguously assigned.[27] This comparison shows that the bond lengths of the tetraselenafulvalene core of the A-type donor molecule in **2** are within the range found for the BETS molecules with a formal charge of +1/2. The ionic charges of the B and C-type molecules in **2** are more difficult to assign since not all the bond distances agree with a unique charge assignment. Nevertheless, we can estimate an average charge near +1/2 for both B and C molecules. Therefore, the whole positive charge in **2** has to be near +4, indicating that the polyoxomolybdate has been reduced by two electrons during the electrocrystallization process, bearing a total charge of −4. Susceptibility and electron spin resonance (ESR) measurements (see below) also agree with the presence of two-electron reduced Keggin anions in **2**, supporting the presence of two-electron reduced anions bearing a charge of −4 and, therefore, the electronic distribution in **2** is assumed to correspond to the anion $[SMo_{12}O_{40}]^{4-}$. Likewise, these magnetic measurements on compound **1** corroborate the presence of one-electron reduced Keggin anions with a charge of −3 in **1**.

(24) Farrugia, L. J. *J. Appl. Crystallogr.* **1997**, *30*, 565.

(25) Guionneau, P.; Kepert, C. J.; Bravic, G.; Chasseau, D.; Truter, M. R.; Kurmoo, M.; Day, P. *Synth. Met.* **1997**, *86*, 1973.

(26) Kurmoo, M.; Day, P.; Bellito, C. *Synth. Met.* **1995**, *70*, 963.

(27) (a) Malfant, I.; Courcet, T.; Faulmann, C.; Cassoux, P.; Gornitzka, H.; Granier, F.; Doublet, M.-L.; Guionneau, P.; Howard, J. A. K.; Kushch, N. D.; Kobayashi, A. *C. R. Acad. Sci., Ser. IIc: Chim.* **2001**, *4*, 149. (b) Pilia, L.; Faulmann, C.; Malfant, I.; Colliere, V.; Mercuri, M. L.; Deplano, P.; Cassoux, P. *Acta Crystallogr., Sect. C: Cryst. Struct. Commun.* **2002**, *58*, m240. (c) Courcet, T.; Malfant, I.; Pokhodnia, K.; Cassoux, P. *New J. Chem.* **1998**, 585. (d) Kobayashi, H.; Tomita, H.; Naito, T.; Kobayashi, A.; Sakai, F.; Watanabe, T.; Cassoux, P. *J. Am. Chem. Soc.* **1996**, *118*, 368.

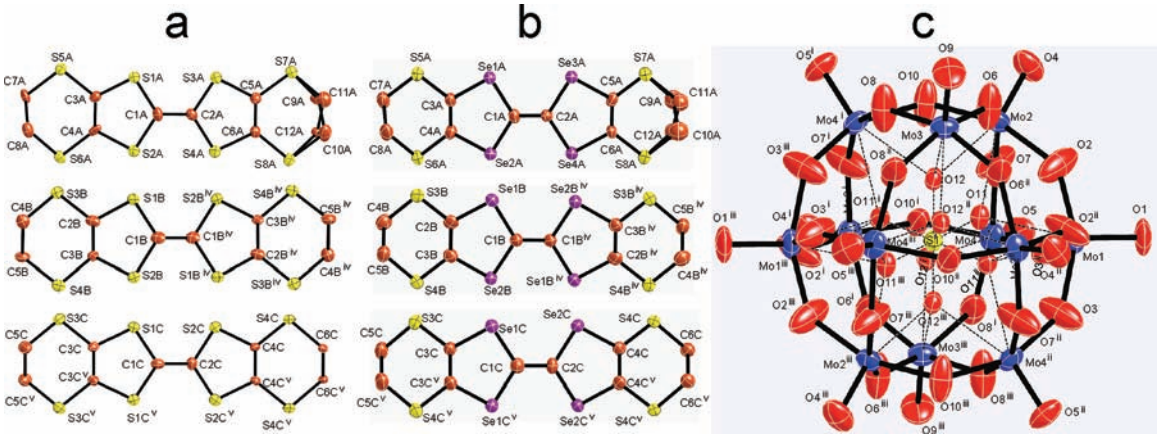

Figure 2. ORTEP diagrams with 50% thermal ellipsoids and atom numbering scheme for the three crystallographycally independent ET molecules in compound **1** (a), the three crystallographycally independent BETS molecules in compound **2** (b), and the Keggin POM in compound **2** (c). Bonds inside the POM cage are depicted as dashed lines in (c) for clarity. The atom numbering scheme for the Keggin POM in compound **1** is similar to that in **2**. Symmetry codes: (i) $-x+1, y, -z+1$; (ii) $x, -y+1, z$; (iii) $-x+1, -y+1, -z+1$; (iv) $-x+3/2, -y+1/2, -z+1/2$; (v) $-x+1, y, -z$.

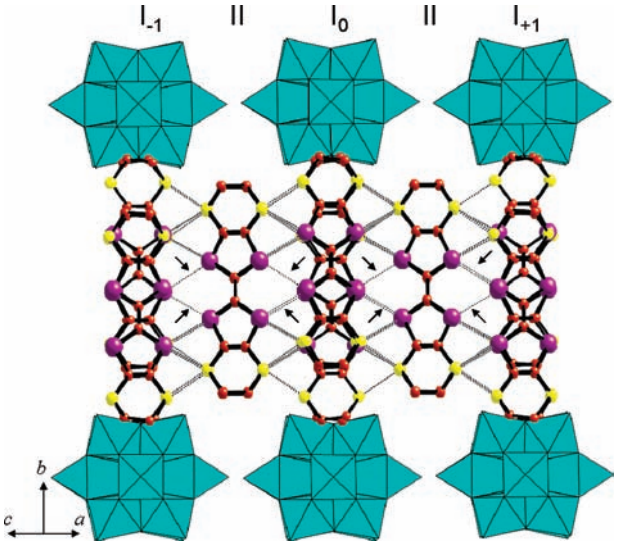

Figure 3. Structure of compound **2** showing the alternating layers of the POM and the BETS molecules and the two different types of organic chains I and II. Dotted lines indicate intermolecular S···S, S···Se, or Se···Se contacts shorter than the sum of the van der Waals radii. Arrows point those short intermolecular contacts that are not found in compound **1** (see text).

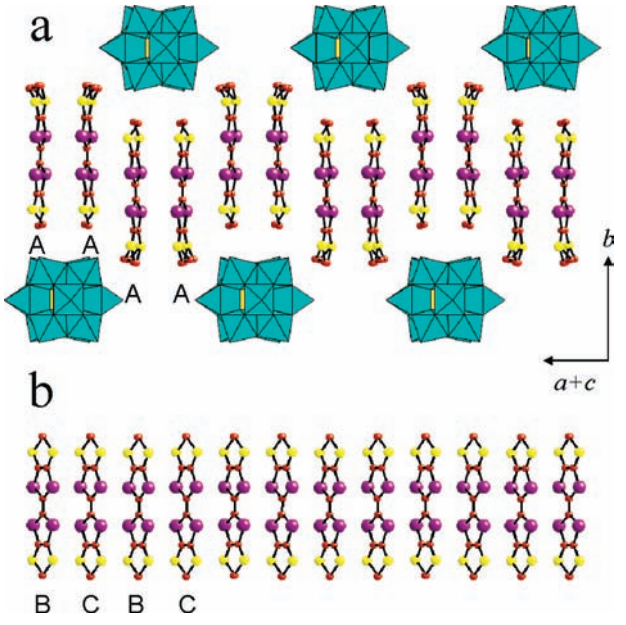

Figure 4. (a) Side view of type I chains in compound **2** showing the zigzag BETS dimers and the coplanar Keggin anions. (b) Side view of type II chains showing the eclipsed packing of the BETS molecules in **2**.

Electrical Properties

The dc electrical conductivity, measured by the four contacts method on several single crystals of the ET salt (**1**) shows an activated conductivity regime in the temperature range 300−100 K with room temperature conductivities of about 1 S cm^{-1} (Figure 5). Below about 100 K the resistivity of all the samples was too high to be measured by our measurement system. The Arrhenius plot of the resistivity (Ln ρ vs $1/T$) of **1** shows a linear dependence in all the temperature range measured (300−100 K) with an activation energy of about 130 meV (inset in Figure 5). The dc electrical properties of **2** also show, as in **1**, an activated conductivity in all the measured temperature range (300−2 K) although with higher room temperature conductivities (in the range 10−60 S cm^{-1}, Figure 6). In contrast to **1**, in **2** the increase of the resistivity when the temperature is decreased is very smooth, and some crystals even show a smooth decrease in the resistivity at about 200−150 K (Figure 6). Thus, the conductivities at 2 K only decrease by a factor of about 10−100 when cooling the sample from 300 to 2 K). This behavior suggests that **2** is a semiconductor with a very small activation energy (this is compatible with the results of band structure calculations suggesting that both localized and delocalized electrons are responsible for the conductivity, see below). In fact, the Arrhenius plot of the resistivity (inset in Figure 6) shows a continuous change in the slope, from high values at high temperatures (in the range 50−140 meV) to very low values at low temperatures (in the range 0.10−0.20 meV). This behavior confirms that the activated conductivity observed in **2** does not follows a classical semiconducting regime, as observed in **1**.

Since the band structure calculations suggest that in **2** there are both localized and delocalized electrons near the Fermi level, we have also performed dc conductivity measurements under pressure to see if the metallic state could be

Table 2. Intermolecular Chalcogen···Chalcogen Distances Shorter than the Sum of the van der Waals Radii[a] in Compounds **1** and **2**[b]

$ET_8[SMo_{12}O_{40}]\cdot 10H_2O$ (**1**)		$BETS_8[SMo_{12}O_{40}]\cdot 10H_2O$ (**2**)	
Contacts Involving Chalcogens of Fulvalene Moieties Only			
		Se(1A)−Se(1B)^{ii}	3.7624(13)
		Se(3A)−Se(2B)^{iii}	3.7593(13)
		Se(4A)−Se(2B)^{iv}	3.7479(13)
Contacts between Chalcogens of Fulvalene Moieties and S Atoms of Dihydrodithiin Rings			
S(6A)−S(1C)^{i}	3.578(5)	S(6A)−Se(1C)^{i}	3.602(3)
S(5A)−S(1B)^{ii}	3.545(5)	S(5A)−Se(1B)^{ii}	3.612(3)
S(5A)−S(2C)^{ii}	3.564(4)	S(5A)−Se(2C)^{ii}	3.550(3)
S(3A)−S(4B)^{iii}	3.560(4)	Se(3A)−S(4B)^{iii}	3.553(3)
S(4A)−S(4B)^{iv}	3.535(4)	Se(4A)−S(4B)^{iv}	3.578(3)
		Se(4A)−S(4C)^{i}	3.663(3)
		Se(3A)−S(3C)^{ii}	3.657(3)
Contacts Involving Sulfur Atoms of Dihydrodithiin Rings Only			
S(7A)−S(4B)^{iii}	3.508(5)	S(7A)−S(4B)^{iii}	3.569(3)
S(8A)−S(4B)^{iv}	3.494(4)	S(8A)−S(4B)^{iv}	3.548(4)
S(8A)−S(4C)^{i}	3.510(5)	S(8A)−S(4C)^{i}	3.591(3)
S(5A)−S(4C)^{ii}	3.399(4)	S(5A)−S(4C)^{ii}	3.459(3)
S(5A)−S(3B)^{ii}	3.518(5)	S(5A)−S(3B)^{ii}	3.595(3)
S(6A)−S(3C)^{i}	3.516(5)	S(6A)−S(3C)^{i}	3.562(4)
S(7A)−S(3C)^{ii}	3.575(5)		

[a] 3.60 Å for S···S, 3.70 Å for S···Se, and 3.80 for Se···Se. [b] Symmetry codes: (i) $-x+1, y, -z+1$; (ii) $x+1/2, -y+1/2, z+1/2$; (iii) $-x+2, y, -z+1$; (iv) $x, y, z+1$.

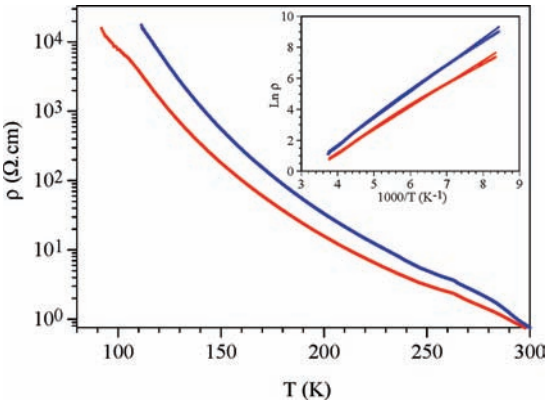

Figure 5. Thermal variation of the electrical resistivity (logarithmic scale) of two different crystals of salt **1**. Inset shows the Arrhenius plot with the linear fit (solid line).

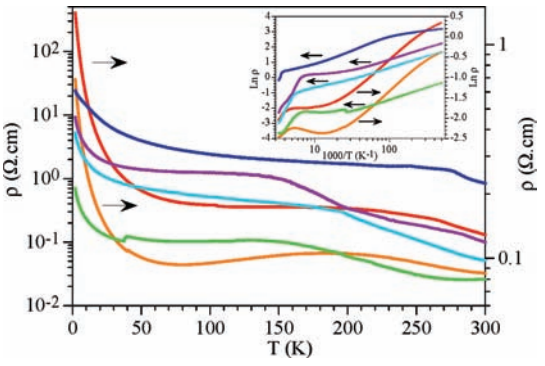

Figure 6. Thermal variation of the electrical resistivity (logarithmic scale) of six different crystals of salt **2**. Inset shows the Arrhenius plot. Note that the abscissa is in a logarithmic scale.

stabilized. Although no transition to the metallic state has been detected for pressures below about 10 kbar, we have observed a significant decrease of the resistivity with increasing pressures (Figure 7).

Magnetic Properties

The product of the magnetic susceptibility times the temperature ($\chi_m T$) for the ET salt (**1**) presents a room temperature value of about 1.5 emu K mol^{-1}, corresponding to the contribution of both the organic and the inorganic sublattices (Figure 8). When the temperature is decreased, the $\chi_m T$ product decreases to reach a plateau of about 0.4 emu K mol^{-1} at low temperatures. This behavior indicates that there is a total contribution of about four electrons with a residual paramagnetism at low temperatures corresponding to about one electron. This contribution may be attributed to the presence of an extra electron in the reduced $[SMo_{12}O_{40}]^{3-}$ POM and, therefore, with a contribution of about three electrons coming from the organic sublattice. These three electrons would present an antiferromagnetic coupling as shown by the thermal variation of the corrected molar susceptibility (inset in Figure 8). Thus, if we correct the magnetic susceptibility of **1** with the contribution of one electron (0.375 emu K mol^{-1} for a g value of 2.0), the resulting corrected susceptibility shows a rounded maximum at about 70 K, confirming the presence of a moderate antiferromagnetic coupling inside the organic sublattice. This result is very similar to that observed in the family of isostructural ET salts with other Keggin POM.[7] Furthermore, the paramagnetic contribution of one unpaired electron found in the reduced $[SMo_{12}O_{40}]^{3-}$ POM is also very similar to that found in the BETS salt of the related, and also reduced, $[PMo_{12}O_{40}]^{4-}$ POM.[12] Moreover, this result also agrees with the proposed charge distribution as obtained from the analysis of the bond distances in the ET molecules (see above) and with the EPR spectra and the band structure calculations (see below).

The thermal variation of the $\chi_m T$ product for the BETS salt (**2**) shows a room temperature value of about 0.12 emu K mol^{-1} that linearly decreases with decreasing temperatures

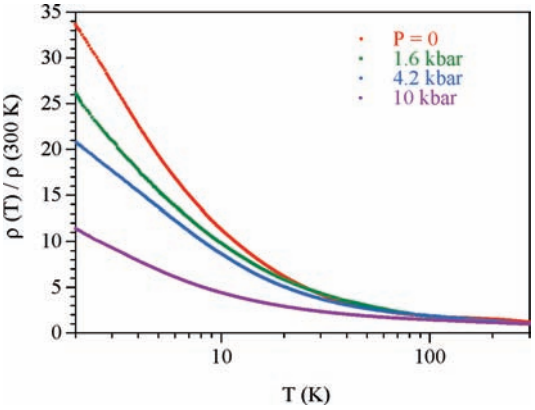

Figure 7. Thermal variation of the normalized electrical resistivity of a single crystal of salt **2** at different pressures. Note that the abscissa is in a logarithmic scale.

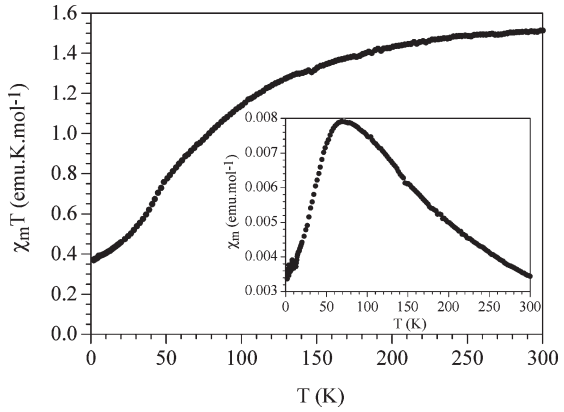

Figure 8. Thermal variation of the $\chi_m T$ product for salt **1**. Inset shows the molar susceptibility of the organic sublattice as obtained when the total susceptibility is corrected with a Curie tail corresponding to the anionic contribution (see text).

to reach a value of about 0.06 emu K mol^{-1} at about 20 K. Below this temperature, $\chi_m T$ shows a more pronounced decrease to reach a value of about 0.036 emu K mol^{-1} at 2 K (Figure 9). This behavior indicates that **2** is essentially diamagnetic, although presents a Pauli-type temperature independent paramagnetic contribution (of ca. 2×10^{-4} emu mol^{-1}, typical of metals and highly conducting materials)[28] and a small paramagnetic contribution, corresponding to about 10−15% of the contribution of a localized electron per formula unit. This result clearly shows that both salts present very different magnetic behaviors and, therefore, that both salts must contain differently reduced anions, in agreement with the estimations made from the bond distances (see above). In **2**, the contribution of about 1/10 electron is also confirmed by the isothermal magnetization at low temperatures, that show a saturation value of about 0.1 μ_B (inset in Figure 9), corresponding to about 1/10 of the expected value for one localized electron, in agreement with the susceptibility measurements. Although the values obtained are not very precise, because of the reduced mass of the measured sample, we can conclude that **2** presents a diamagnetic $[SMo_{12}O_{40}]^{4-}$ anion, in agreement with the estimations from the bond

(28) Williams, J. M; Ferraro, J. R.; Thorn, R. J.; Carlson, K. D.; Geiser, U.; Wang, H. H.; Kini, A. M.; Whangbo, M. H. *Organic Superconductors: Including Fullerene*; Prentice-Hall: Englewood Cliffs, NJ, 1992.

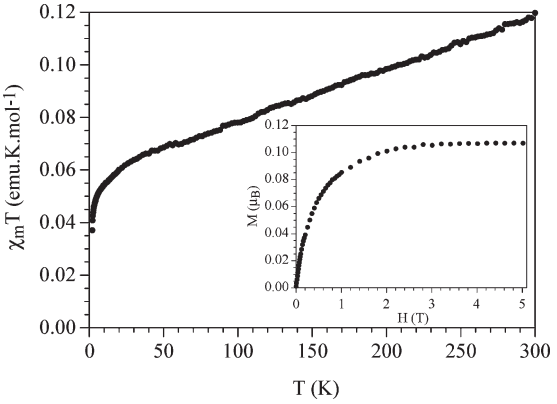

Figure 9. Thermal variation of the $\chi_m T$ product for salt **2**. Inset shows the isothermal magnetization at 2 K.

distances. Note that the two extra electrons of the doubly reduced $[SMo_{12}O_{40}]^{4-}$ anion are expected to present a strong antiferromagnetic coupling, leading to a diamagnetic contribution for this anion.[29] The low paramagnetic contribution may arise from the presence of a small fraction of isolated $BETS^+$ radicals, because of crystal defects, in the organic sublattice and/or to the presence of a small fraction (ca. 10%) of $[SMo_{12}O_{40}]^{3-}$ POMs reduced by only one electron. This result is also in agreement with the EPR results (see below). Besides the inorganic anions, there are also important differences in the magnetic contributions of the organic sublattices in both salts. Thus, in **1** the electrons of the organic sublattice are antiferromagnetically coupled in agreement with their localized character and with previous measurements in similar salts. On the contrary, the electrons of the organic sublattice in salt **2** lead to a Pauli-type paramagnetism, in agreement with their more delocalized character. Unfortunately, given the small amount available of sample **2**, the accuracy of the measurement at high temperatures is not too high, and we cannot determine very accurately the exact value of this contribution.

Electron Spin Resonance

The electron paramagnetic resonance (EPR) spectra of both compounds are quite similar, except for some differences in the donor signals and in the intensity of the signals (Figures 10 and 11). At room temperature the POM is EPR silent since the extra electron in the reduced POM is fully delocalized and, thus, salt **1** presents a symmetrical signal, centered at about 3380 G (g = 2.005) with a line-width of about 31 G arising from the ET organic radicals and typical of 2D ET radical salts (see Supporting Information, Figure S1).[29] When the temperature is decreased, this signal slowly shifts to higher fields (lower g values) down to about 80−90 K (where the g value is ca. 2.003). Below 80 K this signal moves faster to reach a value of about 1.987 at 3 K (Supporting Information, Figure S1). This low value suggests that below about 80 K the signal is distorted by the POM one, arising as a consequence of the partial localization of the extra electron

(29) (a) Borrás-Almenar, J. J.; Clemente, J. M.; Coronado, E.; Tsukerblat, B. S. *Chem. Phys.* **1995**, *195*, 1. (b) Suaud, N.; Gaita-Ariño, A.; Clemente-Juan, J. M.; Sánchez-Marín, J.; Coronado, E. *J. Am. Chem. Soc.* **2002**, *124*, 15134. (c) Suaud, N.; Gaita-Ariño, A.; Clemente-Juan, J. M.; Sánchez-Marín, J.; Coronado, E. *Polyhedron* **2003**, *22*, 2331. (d) Suaud, N.; Gaita-Ariño, A.; Clemente-Juan, J. M.; Coronado, E. *Chem.—Eur. J.* **2004**, *10*, 4041.

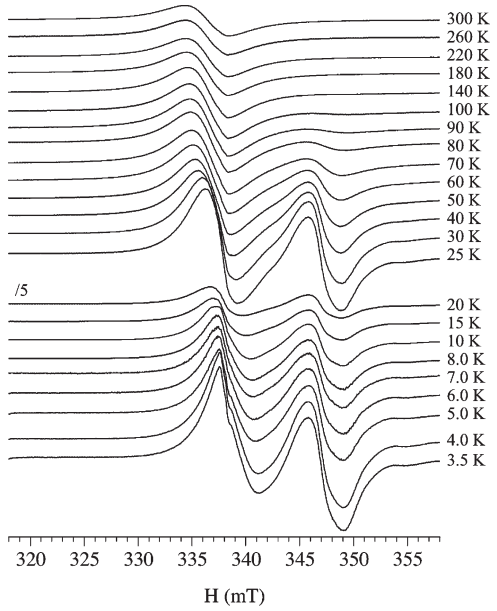

Figure 10. Thermal variation of the X-band EPR spectrum of salt **1** showing the signal associated to the organic sublattice (at ca. 338 mT) and with the reduced POM (at ca. 347 mT).

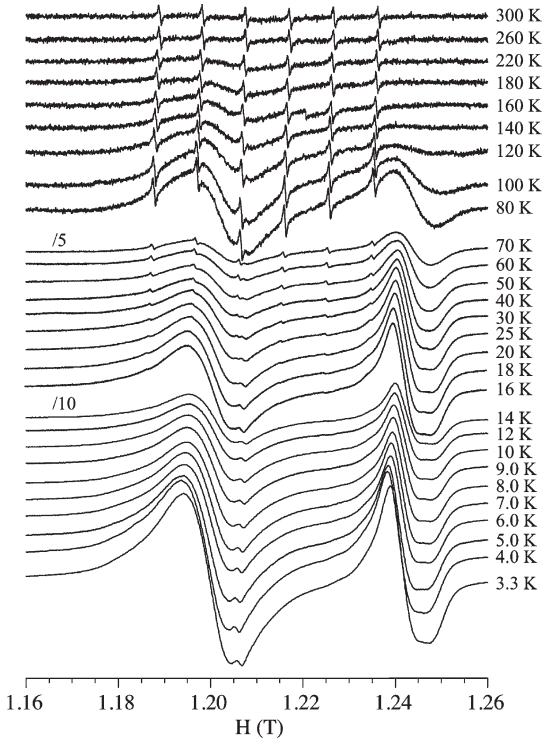

Figure 11. Thermal variation of the Q-band EPR spectrum of salt **2** showing the signal associated with the organic sublattice (at ca. 1.20 T) and with the reduced POM (at ca. 1.24 T). The sextuplet centered at about 1.21 T observed at high temperatures comes from a Mo-containing reduced species present as an impurity.

in the POM (Figure 10). This POM signal is very similar to those observed in other Mo-containing reduced POM.[12,30]

As already mentioned, salt **2** shows a similar behavior (Figure 11) although the BETS signal (at $g = 2.015$, Supporting Information, Figure S2) is only clearly observed below about 180 K, suggesting that only a small fraction of the donor molecules are isolated $BETS^+$ radicals, in agreement with the proposed charge distribution. The BETS signal in **2** (ca. 120 G at high temperatures) is much broader than that of the ET signal in **1**. This fact confirms the higher electronic dimensionality of salt **2**, in agreement with the better overlap of the Se orbitals (as compared with the S ones in salt **1**), with the electrical conductivity measurements and with the band structure calculations (see above).

The POM signal in both salts are almost identical and present identical thermal dependences (Supporting Information, Figure S2), except that in **2** it is much weaker. This results strongly suggests that in both salts the POM signal arises from the same singly reduced $[SMo_{12}O_{40}]^{3-}$ anions and, therefore, that the fraction of $[SMo_{12}O_{40}]^{3-}$ anions is much smaller in **2**, in agreement with the proposed charge distribution and with the magnetic susceptibility measurements.

Finally, the sextuplet observed at high temperatures in the EPR spectra of **2** suggests that there are some isolated Mo(V)-containing impurities showing a hyperfine splitting due to the coupling of the electron with the nuclear spin (^{95}Mo and ^{97}Mo both with $I = 5/2$ and natural abundances of 15.90% and 9.60%, respectively). The more extreme conditions used for the acquisition of the spectra of salt **2** (given its much lower intensity) is also responsible for the detection of this sextuplet, as suggested by the fact that below about 70 K this signal becomes almost negligible.

Band Structure Calculations. To gain some insight into the relationship between the crystal structure and transport properties of the two new salts and, in particular, the question of the charge of the donors, we have carried out tight-binding band structure calculations for the donor layers of both salts. As shown in Figure 1 these donor layers are built from parallel stacks along the $(a + c)$-direction condensed in a typical α-mode. There are three different donor molecules (A, B, and C) and seven different donor···donor interactions (see Figure 12), three of which are intrastack interactions (I to III) and four are interstack interactions (IV to VII). To have a hint on the strength of the interaction between the highest occupied molecular orbital (HOMO) of a given donor and that of a nearest neighbor for the seven different types of intermolecular interactions, we have also calculated the $\beta_{HOMO-HOMO}$ interaction energies.[31] The absolute values of these energies for salts **1** and **2** are reported in Table 3. The calculated band structures in the region of the HOMO-based bands for the two salts are shown in Figure 13. Since there are eight donors per repeating unit, for POM charges between −2 and −4 there must be from two to four holes in these bands.

Even a quick look at these results immediately suggests that the two salts are quite different. For instance, the two upper bands, which are those which would accommodate the holes for POM charges between −2 and −4, are very flat for **1** but considerably more dispersive for **2**. This is consistent with the $\beta_{HOMO-HOMO}$ interaction energies of

(30) (a) Bellitto, C.; Bonamico, M.; Fares, V.; Federici, F.; Righini, G.; Kurmoo, M.; Day, P. *Chem. Mater.* **1995**, *7*, 1475. (b) Prados, R. A.; Pope, M. T. *Inorg. Chem.* **1976**, *15*, 2547. (c) Sánchez, C.; Livage, J.; Launay, J. P.; Fournier, M.; Jeannin, Y. *J. Am. Chem. Soc.* **1982**, *104*, 3194.

(31) Whangbo, M.-H.; Williams, J. M.; Leung, P. C. W.; Beno, M. A.; Emge, T. J.; Wang, H. H. *Inorg. Chem.* **1985**, *24*, 3500.

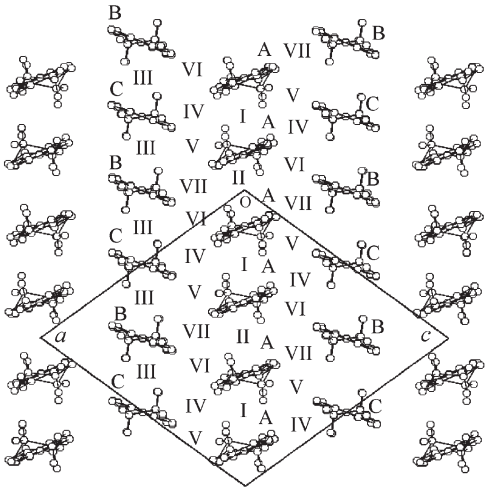

Figure 12. View of the donor layer of salts **1** and **2** along the *b*-direction. The different types of donors (A−C) and donor···donor interactions have been labeled (I−VII).

Table 3. Absolute Values of the $\beta_{HOMO-HOMO}$ Interaction Energies (eV) Calculated for the Different Donor····Donor Interactions in the Donor Lattices of **1** and **2**

	$\lvert\beta_{HOMO-HOMO}\rvert$ (eV)	
interaction[a]	$ET_8[SMo_{12}O_{40}]\cdot 10H_2O$ (**1**)	$BETS_8[SMo_{12}O_{40}]\cdot 10H_2O$ (**2**)
I (A-A)	0.0537	0.0084
II (A-A)	0.1249	0.2064
III (B−C)	0.0251	0.1047
IV (C-A)	0.0635	0.1234
V (C-A)	0.1084	0.1699
VI (B-A)	0.0651	0.1124
VII (B-A)	0.0810	0.1420

[a] See Figure 12.

Table 3 since those for **1** are considerably smaller than those for **2**. It is clear that the HOMO−HOMO interactions in salt **1** are weak and consequently, the carriers, whatever their number, will be localized leading to activated conductivity. It is also clear that salt **2** will be a considerably better conductor because the HOMO−HOMO interactions are stronger.

Analysis of the nature of the bands in Figure 13 shows another important difference between the two systems.[32] In the case of salt **1**, the two lower HOMO bands (see Figure 13a) are largely concentrated on the donors B whereas the other bands are almost equally distributed among donors A and C. In contrast, for salt **2** all bands (see Figure 13b) are delocalized among the three types of donors. This is a key difference because it makes clear that in salt **1** donor B is formally neutral and the charge is shared by donors A and C. In contrast, according to these results the charge must be shared almost equally by the three types of donors in the case of salt **2**, (in agreement with the estimations made from the bond distance data). This analysis is consistent with the fact that the energy of the HOMO of donor B lies considerably lower in energy than those of donors A and C (i.e., $\Delta = 0.22$ and 0.24 eV, respectively) for salt **1** whereas the HOMOs of the three

(32) Even if the system is localized, the band structure gives important information concerning the electronic structure.

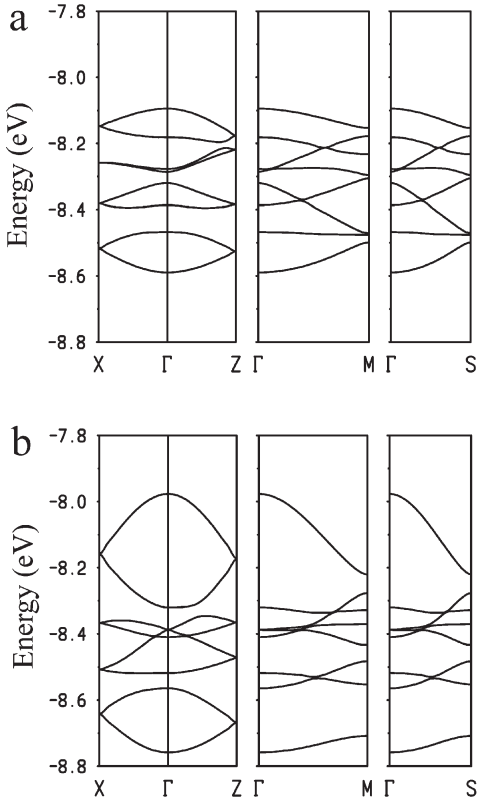

Figure 13. Calculated band structure in the region of the HOMO bands for the donor layers of salts **1** (a) and **2** (b). Γ = (0, 0), X = (a^*/2, 0), Z = (0, c^*/2), M = (a^*/2, c^*/2), and S = (−a^*/2, c^*/2).

donors all lie in a narrow energy range of less that 0.1 eV for **2**. Consequently, the charge distribution must be different in the two salts.

The previous results are in excellent agreement with the structural discussion above and clearly suggest that donors B are neutral in **1**. This means that the three holes must be shared by six donors (four donors A and two donors C) which thus have an average charge of +1/2. It is relatively simple to understand the possible origin of the localization sites as far as donors A are concerned. Since there are four donors in a stack and two different types of interactions, we can consider that these stacks are really a chain of dimers and consequently, that there are two $(A\text{-}A)^{\cdot+}$ dimers. This would take account of two of the three holes per unit cell. This is confirmed by interaction energies of Table 3. Interaction II[33] is the largest in the system and is more than twice larger than the interaction along the stacks (I). The situation is less clear for donors C. These donors are separated by the neutral donors B and thus, it is difficult to understand how two donors C can share a hole. Although analysis of the interactions energies of Table 3 can suggest some discrete units implicating both donors A and C which could accommodate the three localized electrons, we believe that there is only one which does not contradict the structural (geometry of the donors and symmetry of the cell) and electronic information. In this description, one hole is

(33) For salt **1** interaction II is the interaction between the two donors labeled A in Figure 4 and is associated with S···S contacts (<4.0 Å) of 3.838, 3.849 (×2), 3.910, 3.962 (×2), and 3.983 (×2) Å, whereas interaction I is associated with S···S contacts of 3.925 (×2) and 3.958 (×2) Å.

localized in every one of the two $(A\text{-}A)^{\cdot+}$ dimers of the cell, donors B are neutral, and another hole is statistically distributed among the two donors C. Since the X-ray structure can only give a structural average, the sites corresponding to donor C exhibit a structure typical for donors with a formal +1/2 charge.

The situation is very different for salt **2**. In that case, all interactions except I are quite sizable. However, as mentioned, the key observation concerning the electronic structure is that all bands in Figure 13b are delocalized over donors A, B, and C. This means that the HOMO--HOMO interactions between the three types of donors are substantial and quite comparable, ruling out the possibility of having one of the three donor sites fully occupied by neutral molecules, as it was the case for **1**. This brings to the fore the important question of what is actually the charge of the POM. We believe that this charge should be −4. As noted above, given the lattice of these salts, it is not easy to find a convincing description of how three holes are localized in the eight sites of the unit cell when none of the three donors sites is fully occupied with a neutral molecule; but, after all, the system is also semiconducting (though not a usual one) and one should end up with such a description. The situation would be simpler if the POM charge was −4. Examination of the band structure of Figure 13b suggests that a −4 charge is more consistent with the transport properties than a −3 charge. The reason is that for a −3 charge there are three holes in the bands of Figure 13b and the Fermi level for the hypothetical metallic state would cut the quite dispersive upper pair of bands, and the salt would most likely be a metal. With a charge of −4, the Fermi level cuts both the dispersive and the non dispersive bands which overlap just below −8.3 eV (see for instance the Γ → M and Γ → S lines). This means that with four holes per repeating unit there would be both localized and delocalized electrons in the region of the Fermi level. It is quite likely that the atypical but enhanced conductivity behavior of salt **2** arises from the competition among the two types of carriers.

It is also easy to find a localized view of this situation. Note that in salt **2** the difference between interactions II and I is considerably larger than it was in salt **1** (see Table 3). This means that the dimerization in the stacks of donors A is even stronger and thus, their description as a series of $(A\text{-}A)^{\cdot+}$ dimers is even more appropriate now. Let us point out that the central C=C distance of donors A is practically the same in salts **1** (1.361(17) Å) and **2** (1.357(11) Å) providing support for our assignment. Since the stacks of donors B and C are uniform, we believe that the only way to accommodate the two additional holes is to assume that they are statistically distributed between the sites of donors B and C. Note that since donors B are fully neutral in **1**, the charge of donors C is larger (+1/2) than would be the average charge of donors B and C (+1/4) in **2** if the donor layers where equally oxidized. This is at odds with the fact that the central C=C distance of donor C in **1** (1.36(2) Å) is equal or shorter than those of donors B and C in **2** (1.382(16) and 1.369(16) Å, respectively) whereas, as mentioned above, the central C=C distance of donors A is practically the same in both salts. In addition, the central C=C distance in **2** for both donors B and C is longer than it is for donor A which, again, would not agree with a smaller charge for the former. We reach exactly the same conclusions when instead of the central C=C distances we look at the HOMO energies of the different donors.

In short, we believe that there are structural and electronic reasons suggesting that the POM exhibits a −4 charge in salt **2**. Whereas, according to the values of Table 3, the stacks of donors A may be described as chains of localized dimers, the average interaction between donors B and C is quite substantial so that this chain can be described either as a series of interacting $(donor)^0$ and $(donor)^+$ localized units or as a metallic three-quarters filled chain of donors. Since the two types of parallel stacks are coupled through quite sizable interactions it is difficult to predict the outcome of the interaction between the two subsystems: full hole delocalization, and then the metallic description of the system through the band structure of Figure 13b will be appropriate, or weak interaction and localization in the chains of B/C donors, in which case the localized (semiconducting) description would be appropriate. Even an intermediate state with delocalization within the chains of the B/C donors and localization within the chain of donors A is possible. The three situations are most likely competing in **2** and its relative weight changing as a function of temperature and pressure. Whatever the final outcome is, the increase in both the number of holes and strength of the interactions compared with the situation in salt **1** certainly provides a strong bias toward the stabilization of the metallic state, as well as an increase of the conductivity in the localized state. Although use of pressures up to 10 kbar have not been enough to stabilize the metallic state of **2** for a broad temperature range (note that the possible existence of a small fraction of POM with a −3 charge suggested above, provides a weak but non-negligible inhomogeneous field somewhat hindering the stabilization of the metallic state), we believe that in view of the previous discussion this goal should be attainable. It would also be very interesting to see if isostructural ET and BETS salts with slightly different POMs could be prepared in such a way that the possibility of full occupation of the B and C donor sites could be changed and examine the influence on the transport properties.

Conclusions

We have prepared and characterized for the first time a salt in the ET_8[Keggin]·solvent series (**1**) where the Keggin POM ($[SMo_{12}O_{40}]^{3-}$ in this case) presents an anionic charge lower than 4. This result enlarges the range of anionic charges of the POMs used in this series (from −3 to −6) and allows a better control of the band filling of the organic sublattices. Unfortunately, the present case, where the charge is −3 presents a semiconducting behavior because of the inhomogeneous charge distribution among the three crystallographically independent ET donors (as was the case in the other derivatives with charges between −4 and −6). The BETS salt (**2**), on the other side, represents the only example of a radical salt with a doubly reduced POM ($[SMo_{12}O_{40}]^{4-}$ in this case) and the first radical salt of the donor BETS with any POM. The use of this selenium-containing donor has allowed obtaining a highly conducting radical salt, in agreement with the better overlap expected for this donor as compared with the ET

donor. Furthermore, this is the first hybrid radical salt where such high electron delocalization is found in both the organic and the inorganic sublattices. Conductivity measurements under pressure show an improvement of the conductivity and a decrease in the activation energy, in agreement with the band structure calculations. Although no metallic behavior has been observed below 10 kbar, we are convinced that measurements under higher pressures may lead to a metallic state in a large temperature range in this salt.

Acknowledgment. We acknowledge the European Union (MAGMANet network of excelence and European Research Council (Advanced Grant SPINMOL), the Spanish Ministerio de Educación y Ciencia (Projects MAT2007-61584, CSD 2007-00010 Consolider-Ingenio in Molecular Nanoscience, CTQ2008-06720-C02-01/BQU and FIS2006-12117-C04-01) and the Generalitat Valenciana (Project PROMETEO/2009/095) for financial support.

Supporting Information Available: Figures S1 and S2, showing the thermal variation of the EPR parameters of both salts. Crystallographic information files (CIF) for compounds **1** and **2**. This material is available free of charge via the Internet at http://pubs.acs.org.